

## Behavior of nitrogen atoms in SiC-SiO<sub>2</sub> interfaces studied by electrically detected magnetic resonance

T. Umeda,<sup>1(a)</sup> K. Esaki,<sup>1</sup> R. Kosugi,<sup>2</sup> K. Fukuda,<sup>2</sup> T. Ohshima,<sup>3</sup> N. Morishita,<sup>3</sup> and J. Isoya<sup>4</sup>

<sup>1</sup>*Institute of Applied Physics, University of Tsukuba, Tsukuba 305-8573, Japan*

<sup>2</sup>*National Institute of Advanced Industrial Science and Technology (AIST), Tsukuba 305-8568, Japan*

<sup>3</sup>*Japan Atomic Energy Agency (JAEA), Takasaki 370-1292, Japan*

<sup>4</sup>*Graduate School of Library, Information, and Media Studies, University of Tsukuba, Tsukuba 305-8550, Japan*

(Received 8 June 2011; accepted 6 September 2011; published online 4 October 2011)

The microscopic behavior of nitrogen atoms in the SiO<sub>2</sub>-SiC interface regions of *n*-channel lateral 4H-SiC metal-oxide-semiconductor field effect transistors (MOSFETs) was studied using low-temperature electrically detected magnetic resonance spectroscopy and other techniques. The results show that nitrogen atoms eliminated shallow interface states observable at 20 K and further diffused into the channel region of the MOSFETs as shallow donors. These two behaviors enable nitrogen atoms to change the channel conductivity of SiC MOSFETs. © 2011 American Institute of Physics. [doi:10.1063/1.3644156]

Nitrogen and hydrogen are well known as useful elements for controlling SiC-SiO<sub>2</sub> interfaces.<sup>1</sup> Determining how to make better use of these atoms is crucial for SiC device technologies, especially in terms of improving the channel mobility of SiC metal-oxide-semiconductor (MOS) field effect transistors (MOSFETs).<sup>2,3</sup> Similarly to the well-studied Si-SiO<sub>2</sub> interfaces,<sup>4</sup> dangling-bond (DB) defects were found at SiC-SiO<sub>2</sub> interfaces (on carbon atoms) (Ref. 5) and their reaction with hydrogen atoms was observed in oxidized porous-SiC.<sup>6</sup> Also, it was demonstrated that nitrogen atoms eliminated the *g* (*g* value) = 2.003 center<sup>7</sup> originating from silicon-vacancy defects in the interface region.<sup>7-9</sup> Such elimination is the key to modifying the MOSFETs performance.<sup>9</sup> However, microscopic behaviors of nitrogen at the interface may be more complicated. For example, the incorporation of nitrogen into the interface affects on not only the channel mobility, but also the threshold voltage (*V*<sub>th</sub>).<sup>10</sup> Furthermore, the low channel mobility may originate from both the high interface-state density and other scattering mechanisms.<sup>11</sup> We wonder if there might be still unknown behaviors of nitrogen at the interface.

In this letter, we applied low-temperature electrically detected magnetic resonance (EDMR) spectroscopy to SiC-SiO<sub>2</sub> interfaces in fully processed 4H-SiC MOSFETs. The EDMR technique has been already applied to this interface system in real MOSFET devices and has succeeded to detect electron spin resonance (ESR) signals in the interface region.<sup>7-9</sup> These studies were demonstrated at room temperature (RT). On the contrary, our EDMR studies were performed at low temperatures (down to 4 K). Since many ESR signals, related to shallow energy levels or associated with thermal activation process, become observable at low temperatures, our observation expectedly detects shallow interface states that are located close to the conduction band edge (*E*<sub>C</sub>). In fact, we found that nitrogen atoms that have incorporated into the interface can remove some of the shallow interface defects that interact with the channel current and even diffuse into the channel region as shallow donors.

These donors have an important role for changing the channel conductivity of SiC MOSFETs.

The samples we studied were *n*-channel lateral 4H-SiC MOSFETs [gate length (*L*): 100 μm, gate width (*W*): 150 μm] fabricated on epitaxial layers of Cree 8°-off 4H-SiC(0001) Si-face wafers. Aluminum implantation (Al concentration ≈ 1 × 10<sup>20</sup> cm<sup>-3</sup>) was carried out over the channel region of the *n*-type epitaxial layer (residual nitrogen concentration ≈ 5 × 10<sup>15</sup> cm<sup>-3</sup>). Source/drain regions were formed by high-dose phosphorus implantation (P concentration ≈ 1 × 10<sup>20</sup> cm<sup>-3</sup>) and connected to nickel ohmic contacts. Gate oxides (60 nm in thickness) were grown by dry oxidation and were subjected to post-nitridation annealing (NO-N<sub>2</sub>O at 1250 °C). Gate electrodes were formed by poly-Si. Finally, two 4H-SiC MOSFET samples, named “Nitrogen” and “Dry” (dry oxidation only, oxide thickness = 50 nm), were prepared for the EDMR measurements. Their field-effect channel mobility (*μ*<sub>FE</sub>) is evaluated in Fig. 1(a).

Figure 2 shows a summary of EDMR measurements for our MOSFET samples. EDMR spectra were measured using lateral channel currents (*I*<sub>ds</sub>) between the source and drain of each MOSFET in the dark. The observed EDMR centers should be interacting with the channel currents. The currents *I*<sub>ds</sub> were 1–100 nA under drain-source biases (*V*<sub>ds</sub>) of 1–5 V and gate-substrate biases (*V*<sub>gs</sub>) of 1–30 V at 4–295 K [see Fig. 1(b)]. The *V*<sub>gs</sub> over 30 V was not available because of large gate leakage currents. To excite ESR transition, we used a Bruker Bio-Spin TE<sub>011</sub> microwave cavity and a 9.4-GHz microwave at a power of 32–200 mW. Then, we measured ESR-induced changes in *I*<sub>ds</sub> (expressed in ppm) using a lock-in amplifier which synchronized with magnetic-field modulation at 1.56 kHz.

As shown in Figs. 2(a) and 2(b), RT EDMR signals such as interface signals of the silicon-vacancy and the dangling-bond centers<sup>7-9</sup> were not observed in our MOSFETs. In Fig. 1(c), EDMR signal intensities (peak-to-peak intensities in the EDMR spectra) are plotted for each experiment. At 295 K, any defect signals were below the noise level. As decreasing the temperature, we could detect a low-temperature EDMR

<sup>a)</sup>Electronic mail: umeda@bk.tsukuba.ac.jp.

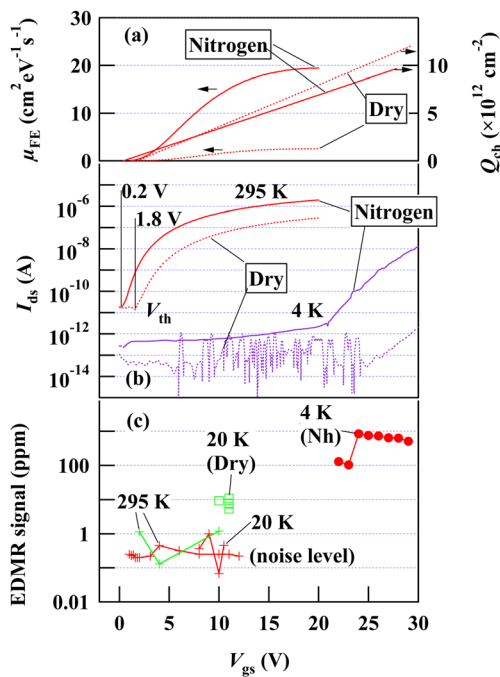


FIG. 1. (Color online) Electrical properties and EDMR signal intensities of Nitrogen and Dry 4H-SiC MOSFET samples. (a) Field-effect mobility (left axis) of MOSFETs derived from room-temperature  $I_{ds}$ - $V_{gs}$  curves, and simulation (right axis) for carrier concentrations ( $Q_{ch}$ ) of the channel, where  $C_{ox} = 7.0 \times 10^{-8}$  F/cm<sup>2</sup> and  $V_{th} = 1.8$  V for the Dry sample and  $C_{ox} = 6.9 \times 10^{-8}$  F/cm<sup>2</sup> and  $V_{th} = 0.2$  V for the Nitrogen sample. These  $C_{ox}$  values were determined by MOS capacitors on the same wafer as the MOSFET samples. (b)  $I_{ds}$ - $V_{gs}$  curves measured for  $V_{ds} = 0.1$  V at 295 K and 1 V at 4 K. (c) EDMR signal intensities (peak-to-peak heights in EDMR spectra) of the Nitrogen (circles) and Dry (squares) samples. “+” symbols represent noise levels of each measurement at which no EDMR signals were detected.

signal at 20 K in the Dry sample [Figs. 1(c)]. This signal was similar to the  $P_{H0}$  signal,<sup>12</sup> but its identification is not decisive. In addition, a broad “unidentified” signal seemed to appear in the Dry sample. This signal may involve a powder pattern owing to randomly orientated defects. In the Nitrogen sample, these signals were not found [Figs. 1(c), 2(d) and 2(g)]. As similarly to the earlier EDMR results at RT,<sup>7–9</sup> nitrogen atoms also annihilated low-temperature EDMR signals. This behavior is an important role of nitrogen, as already discussed in the earlier work.<sup>9</sup> Furthermore, even after  $\gamma$ -ray irradiation [Fig. 2(e)], the Nitrogen samples did not show any EDMR signals. This behavior is in contrast to the case of hydrogen, in which hydrogen removal was observed by  $\gamma$ -ray irradiation.<sup>12</sup> Therefore, nitrogen atoms formed stable binding states at the interface.

We found another significant behavior of nitrogen in the interface region. In the Nitrogen sample, a very strong EDMR signal was observed at 4 K [Figs. 2(f) and 2(h)], which we label “Nh.” The angular dependence of the Nh signal, shown in Fig. 3, reveals a  $c$ -axial ( $C_{3v}$ ) symmetry with  $g_{||} = 2.0047$  and  $g_{\perp} = 2.0008$ , which is similar to the case of nitrogen shallow donors at the carbon  $h$  site of 4H-SiC [ $N_C(h)$ ;  $C_{3v}$  symmetry,  $g_{||} = 2.0055$ , and  $g_{\perp} = 2.0010$ ].<sup>13</sup> Although triplet hyperfine splitting (hfs) of <sup>14</sup>N nucleus ( $I = 1$ , natural abundance = 100%) was not resolved, this behavior is frequently seen for  $N_C(h)$ , because of small <sup>14</sup>N hfs (0.2 mT,<sup>13</sup> see Fig. 3). Judging from the signal width of Nh (0.4–0.5 mT, slightly angular-dependent, cf. Fig. 3), <sup>14</sup>N hfs is at least much smaller than 0.4 mT for the Nh center. This range is

one-tenth smaller than the case of  $k$ -site shallow nitrogen donors,  $N_C(k)$  (3.6 mT,<sup>13</sup> see Fig. 3), implying that both the  $N_C(h)$  and Nh centers are associated with shallower donor states. Also note that observable temperature (<20 K) are in agreement between  $N_C(h)$  and Nh. Therefore, we concluded that the Nh signal originates from the  $h$ -site nitrogen shallow donors in the channel region. The Nh signal exhibited a strong lifetime broadening and disappeared above 20 K [cf. Fig. 2(h)]. Thermal activation energy for this lifetime broadening ( $\Delta E$ ), which was estimated using a signal-width analysis,<sup>14</sup> was 3 meV for the Nh center [Fig. 2(i)]. This value is about half of the reported value (7.6 meV) for  $N_C(h)$ . Thus, shallow donors appear to be quantitatively different in the channel regions and bulk regions. Such a difference is also seen in their  $g$  values. Interestingly, we could not observe  $k$ -site nitrogen donors in the channel currents, despite their ESR signal being more easily detectable over a wide temperature range ( $\leq 80$  K). The reason for this is unclear but may be related to their deeper energy level ( $E_C - 0.09$  eV) compared to that of  $N_C(h)$  ( $E_C - 0.05$  eV).

The above result indicates that nitrogen atoms can diffuse not only into the oxide layer, but also into the SiC substrate after post-nitridation annealing. In fact, the Nitrogen sample showed an enhanced channel current at low temperatures, as shown in Fig. 1(b). At 4 K, it could activate a channel current at  $V_{gs} \geq 21$  V, while the Dry sample could not at the same temperature. This enhanced channel current easily accounts for the “nitrogen doping” in the channel region. Moreover, the Nh signal intensity was so intense [ $\sim 1000$  ppm, see Fig. 1(c)] as compared to the defect signals at 20 K in the Dry sample ( $\sim 10$  ppm), which suggests a substantial level of nitrogen doping. Actually, we have measured the “doped” nitrogen atoms by means of x-ray photoemission spectroscopy (XPS), and although those results will be presented in our separate paper,<sup>15</sup> we would like to reiterate a key point here. In this study, we prepared “Nitrogen” and “Dry” wafer samples similarly to the corresponding Nitrogen and Dry MOSFET samples. Then, after completely etching the oxide layer with a diluted hydrofluoric acid, we measured the XPS spectra of the two wafer samples. In both the Nitrogen and Dry wafer samples, oxygen peaks due to the oxide layer were eliminated after the etching. However, in the Nitrogen wafer sample, nitrogen peaks were still clearly detectable, in addition to silicon and carbon peaks of the substrate. On the basis of this observation, we estimated the nitrogen concentration in the substrate to be in the order of  $10^{14}$  cm<sup>-2</sup>.<sup>15</sup> These nitrogen atoms partly changed into shallow donors by high-temperature annealing during the nitridation process, finally appearing as the Nh center.

We evaluated the effect of such high-density nitrogen donors in the channel region on the electrical properties of MOSFETs. In principle, nitrogen donors should increase the carrier concentration ( $Q_{ch}$ ) of the channel and simultaneously decrease  $V_{th}$  of a MOSFET via the compensation of acceptor concentration ( $N_A$ ) in the channel (cf.  $V_{th} \propto N_A^{1/2}$  (Ref. 16)). In fact, a decrease was observed from 1.8 V to 0.2 V [Fig. 1(b)]. Such a  $V_{th}$  drop is a common phenomenon for the case of nitrogen,<sup>10</sup> and our findings gives a reason for this phenomenon.

The nitrogen donors also influence on the channel conductivity, which depends on both  $Q_{ch}$  and  $\mu_{FE}$ . In general,  $\mu_{FE}$

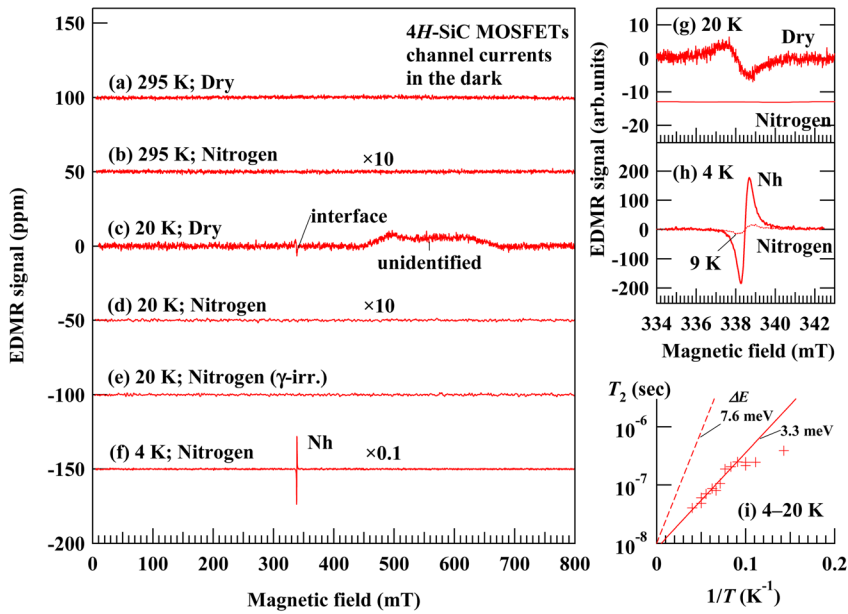


FIG. 2. (Color online) EDMR spectra measured for the channel currents of Nitrogen and Dry 4H-SiC MOSFET samples. (a) Dry sample for  $I_{ds} = 12$  nA for  $V_{ds} = 2$  V,  $V_{gs} = 2$  V, and  $ma = 1$  mT, (b) Nitrogen sample for  $I_{ds} = 41$  nA for  $V_{ds} = 2$  V,  $V_{gs} = 0.3$  V, and  $ma = 2$  mT, (c) and (g) Dry sample for  $I_{ds} = 17$ –23 nA,  $V_{ds} = 2$  V,  $V_{gs} = 11$  V, and  $ma = 1$ –2 mT, (d) and (g) Nitrogen sample for  $I_{ds} = 51$  nA for  $V_{ds} = 2$  V,  $V_{gs} = 10$  V, and  $ma = 1.9$  mT, (e) Nitrogen sample after  $\gamma$ -ray irradiation (average energy = 1.3 MeV, dose = 2.3 Mrad) for  $I_{ds} = 49$  nA for  $V_{ds} = 2$  V,  $V_{gs} = 10$  V, and  $ma = 2$  mT, (f) and (h) Nitrogen sample for  $I_{ds} = 8$ –28 nA,  $V_{ds} = 2$  V,  $V_{gs} = 25$ –27 V, and  $ma = 0.14$ –0.25 mT, where  $ma$  is a magnetic-field modulation amplitude, and all spectra were measured for  $\mathbf{B}$  (magnetic field)  $\parallel$  [0001]. (i) Lifetime broadening behavior of the Nh signal, where  $T_2$  is a spin relaxation time estimated from a lifetime broadening analysis (Ref. 14). Activation energy  $\Delta E$  generally corresponds to a valley-orbit splitting of shallow donor [ $\Delta E = 7.6$  meV for  $N_C(h)$  and 45.5 meV for  $N_C(k)$ ] (Ref. 13).

is determined from the slope of a  $I_{ds}$ - $V_{gs}$  curve via an equation,  $dI_{ds}/dV_{gs} = \mu_{FE} \times C_{ox} \times V_{ds}/(L/W)$ ,<sup>17</sup> in which  $C_{ox}$  is an oxide capacitance. Note that the slope  $dI_{ds}/dV_{gs}$  is increased when  $\mu_{FE}$  or  $C_{ox}$  or  $Q_{ch}$  increases, since  $C_{ox}$  is linked with  $Q_{ch}$  via  $Q_{ch} = C_{ox} \times (V_{gs} - V_{th})$ . Figure 1(a) (right axis) shows the simulated  $Q_{ch}$  in the inversion layer of the MOSFETs using the measured  $C_{ox}$  and  $V_{th}$  values. As shown in this simulation,  $Q_{ch}$  ( $\sim 10^{12}$  cm<sup>-2</sup>) is much smaller than free carriers ( $\leq 10^{14}$  cm<sup>-2</sup>) emitted from the “doped” nitrogen donors. Therefore, it is quite possible that  $Q_{ch}$  is easily enhanced by a factor of tens due to the nitrogen doping, or alternatively, the  $\mu_{FE}$  is overestimated by the same factor. Furthermore, the increased  $Q_{ch}$  may increase the “Coulomb” mobility.<sup>11</sup> These provide an explanation as to how the channel conductivity was improved by nitrogen. Actually, the enhancement by a factor of 7–64 was observed for  $V_{gs} \geq 1.8$  V in the  $\mu_{FE}$  of our Nitrogen and Dry samples [Fig. 1(a)], which is within the expected range of our model. On the contrary, the doped nitro-

gen donors may act as a source of the surface roughness scattering<sup>11</sup> via their surface potential fluctuation. Accordingly,  $\mu_{FE}$  may balance with the opposite mechanisms of the nitrogen donors.

In summary, we studied the microscopic behavior of nitrogen in the interface region of 4H-SiC MOSFETs. Low-temperature EDMR measurements revealed that the nitrogen atoms have two primary behaviors: (1) the removal of shallow interface states detectable at 20 K and (2) the nitrogen doping to the channel region. Due to these behaviors, the channel conductivity of SiC MOSFETs can be increased after post-nitridation annealing. The post-nitridation technique for SiC MOSFETs must be optimized to make better use of these two behaviors of nitrogen.

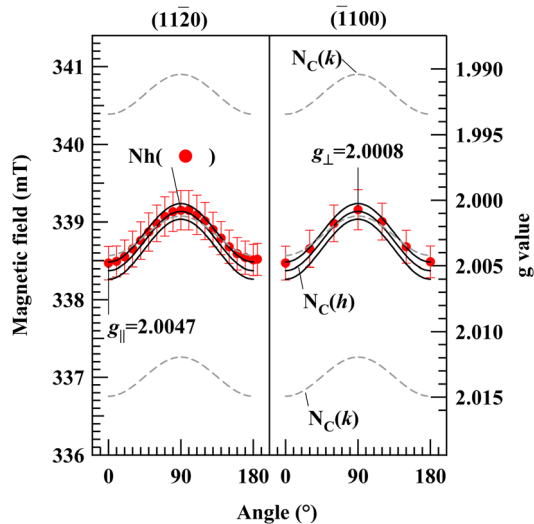


FIG. 3. (Color online) Angular maps of the Nh center (circles) and two nitrogen shallow donors,  $N_C(h)$  (solid lines) and  $N_C(k)$  (dashed lines). Error bars of Nh represent its peak-to-peak signal widths. Two angular maps were measured with respect to the  $\mathbf{B}$  rotation in the  $(11\bar{2}0)$  and  $(\bar{1}100)$  planes, where 0° angle represents that  $\mathbf{B} \parallel$  [0001].

- <sup>1</sup>S. Wang, S. Dhar, S. Wang, A. C. Ahyi, A. Franceschetti, J. R. Williams, L. C. Feldman, and S. T. Pantelides, *Phys. Rev. Lett.* **98**, 026101 (2007).
- <sup>2</sup>V. V. Afanas'ev, A. Stesmans, F. Ciobanu, G. Pensl, K. Y. Cheong, and S. Dimitrijević, *Appl. Phys. Lett.* **82**, 568 (2003).
- <sup>3</sup>K. Fukuda, S. Suzuki, T. Tanaka, and K. Arai, *Appl. Phys. Lett.* **76**, 1585 (2000).
- <sup>4</sup>P. M. Lenahan and J. F. Conley, Jr., *J. Vac. Sci. Technol. B* **16**, 2134 (1998).
- <sup>5</sup>J. L. Cantin, H. J. von Bardeleben, Y. Shishkin, Y. Ke, R. P. Devaty, and W. J. Choyke, *Phys. Rev. Lett.* **92**, 015502 (2004).
- <sup>6</sup>J. L. Cantin, H. J. von Bardeleben, Y. Ke, R. P. Devaty, and W. J. Choyke, *Appl. Phys. Lett.* **88**, 092108 (2006).
- <sup>7</sup>D. J. Meyer, N. A. Bohna, P. M. Lenahan, and A. Lelis, *Mater. Sci. Forum* **457–460**, 477 (2004).
- <sup>8</sup>M. S. Dautrich, P. M. Lenahan, and A. J. Lelis, *Appl. Phys. Lett.* **89**, 223502 (2006).
- <sup>9</sup>C. J. Cochrane, P. M. Lenahan, and A. J. Lelis, *J. Appl. Phys.* **109**, 014506 (2011).
- <sup>10</sup>A. Agarwal, A. Burk, R. Callanan, C. Capell, M. Das, S. Haney, B. Hull, C. Jonas, M. O. Loughlin, M. O. Neil, J. Palmour, A. Powell, J. Richmond, S.-H. Ryu, R. Stahlbush, J. Sumakeris, and J. Zhang, *Mater. Sci. Forum* **600–603**, 895 (2009).
- <sup>11</sup>K. Matocha and V. Tilak, *Mater. Sci. Forum* **679–680**, 318 (2011).
- <sup>12</sup>T. Umeda, K. Esaki, J. Isoya, R. Kosugi, K. Fukuda, N. Morishita, and T. Ohshima, *Mater. Sci. Forum*, **679–680**, 370 (2011).
- <sup>13</sup>S. Greulich-Weber, *Phys. Status Solidi B* **210**, 415 (1998).
- <sup>14</sup>T. Umeda, J. Isoya, N. Morishita, T. Ohshima, T. Kamiya, A. Gali, P. Deak, N. T. Son, and E. Janzen, *Phys. Rev. B* **70**, 235212 (2004).
- <sup>15</sup>R. Kosugi, T. Umeda, and Y. Sakuma, unpublished.
- <sup>16</sup>S. M. Sze and K. K. Ng, *Physics of Semiconductors Devices*, 3rd ed. (Wiley, New Jersey, 2007), Chap. 6.
- <sup>17</sup>S. Harada, R. Kosugi, J. Senzaki, W.-J. Cho, K. Fukuda, K. Arai, and S. Suzuki, *J. Appl. Phys.* **91**, 1568 (2002).